

Battery Energy Storage Station (BESS)-Based Smoothing Control of Photovoltaic (PV) and Wind Power Generation Fluctuations

Xiangjun Li, *Senior Member, IEEE*, Dong Hui, and Xiaokang Lai

Abstract—The battery energy storage station (BESS) is the current and typical means of smoothing wind- or solar-power generation fluctuations. Such BESS-based hybrid power systems require a suitable control strategy that can effectively regulate power output levels and battery state of charge (SOC). This paper presents the results of a wind/photovoltaic (PV)/BESS hybrid power system simulation analysis undertaken to improve the smoothing performance of wind/PV/BESS hybrid power generation and the effectiveness of battery SOC control. A smoothing control method for reducing wind/PV hybrid output power fluctuations and regulating battery SOC under the typical conditions is proposed. A novel real-time BESS-based power allocation method also is proposed. The effectiveness of these methods was verified using MATLAB/SIMULINK software.

Index Terms—Adaptive smoothing control, battery energy storage station (BESS), solar power generation, state of charge (SOC), wind power generation.

NOMENCLATURE

Modeling of Power Sources:

WPGS	WP generation system.
PVGS	PV power generation system.
V_{bat}	Terminal voltage of battery energy storage system (V).
I_{bat}	Current of battery energy storage system (A).
V_{ocv}	Open circuit voltage of battery (V).
$R_{\text{bat}}^{\text{int}}$	Internal resistance of battery energy storage system (Ω).
R_{ch}	Internal resistance of charge (Ω).

R_{dis}	Internal resistance of discharge (Ω).
SOC	State of charge (%).
SOC_{ini}	Initial value of SOC (%).
η	Charging/discharging efficiency (%).
η_{ch}	Efficiency of charge (%).
η_{dis}	Efficiency of discharge (%).
Q_{bat}	Battery energy storage system capacity (kWh).

SOC-Based Smoothing Control Strategy:

u_i	Start–stop status of unit i .
SOC_i	SOC of unit i (%).
SOD_i	State of discharge of unit i (%).
L	Total number of PCS.
M	Total numbers of violating the maximum allowable power limit constraints.
T	Investigated time period (Sec).
n	Number of samples.
Δt	Control cycle (Sec).
$\hat{P}_j^{\text{maxdisch}}$	Allowable maximum discharge power of unit j (kW).
\hat{P}_j^{maxch}	Allowable maximum charge power of unit j (kW).
δ_{WPPV}	Appointed power fluctuation rate limit value (%/min).
A_i	Modified power factor for unit i .
SOC_{ref}	Reference value of SOC (%).
$\text{SOC}_i^{\text{max}}$	Allowable maximum SOC of unit i (%).
$\text{SOC}_i^{\text{min}}$	Allowable minimum SOC of unit i (%).
f_{LT}	A one-dimensional lookup table (LT) block for which the input is the battery SOC_i and the output is A_i .
f_{WPPV}	A function to calculate original wind and PV power fluctuation rate.
f_{hybrid}	A function to calculate wind/PV/BESS hybrid power fluctuation rate.
$r_{(\text{WPPV})}^T$	Original wind and PV generation power fluctuation rate during the investigated time period T (%/min).

Manuscript received May 22, 2011; revised July 25, 2012; accepted February 01, 2013. Date of publication March 07, 2013; date of current version March 18, 2013. This work was supported by the National Natural Science Foundation of China (Grant 51107126): Study on smoothing control strategies for wind/PV power generation based on multitypes large capacity battery energy storage systems, by Key Projects in the National Science and Technology Pillar Program (Grant 2011BAA07B07), and by the National Program on Key Basic Research Project (973 Program) (Grant 2010CB227206). The daily renewable energy data was obtained from the national wind/PV/storage/transmission demonstration power plant located in Zhangbei, Hebei Province, China. (Corresponding author: X. Li.)

The authors are with the Electrical Engineering and New Material Department, China Electric Power Research Institute, Beijing, 100192, China, China (e-mail: lixiangjun@epri.sgcc.com.cn; li_xiangjun@126.com).

Color versions of one or more of the figures in this paper are available online at <http://ieeexplore.ieee.org>.

Digital Object Identifier 10.1109/TSTE.2013.2247428

$r_{(\text{hybrid})}^T$	Wind/PV/BESS hybrid power fluctuation rate during the investigated time period T (%/min).
$P_{(\text{WPPV})}^{\max}$	Maximum power value (KW).
$P_{(\text{WPPV})}^{\min}$	Minimum power value (KW).
$P_{(\text{WPPV})}^{\text{rated}}$	Total rated power of wind and PV generation (KW).
u_k^{WP}	Start-stop status of WPGS k .
u_k^{PV}	Start-stop status of PVGS k .
$P_{\text{WP}_k}^{\text{rated}}$	Rated power of the WPGS k (KW).
$P_{\text{PV}_k}^{\text{rated}}$	Rated power of the PVGS k (KW).
$P_{\text{BESS}}^{\text{ini}}$	Initial power of the BESS (KW).
P_{WPPV}	Total power of WP and PV generation (KW).
T_{WPPV}	Time constant for smoothing control (Sec).
s	Complex variable.
$r_{\text{WPPV}}(t)$	Original total power fluctuation rate of PV and WP generation at time t (%/min).
$K_{\text{WPPV}}^{\text{rise}}$	Rise rate limit value (kW/Sec).
$K_{\text{WPPV}}^{\text{drop}}$	Drop rate limit value (kW/Sec).
$P_{\text{WPPV}}^{\text{DRL}}$	Output power for the proposed dynamic rate limiter (DRL) (KW).
PCS	Power converter systems.
P_i	Target power of PCS i (kW).
P_{BESS}	Target power of the BESS (kW).
$P_{\text{WPPV}}^{\text{smooth}}$	Target smoothing power (kW).
δ_{WPPV}	Appointed power fluctuation rate limit value.

I. INTRODUCTION

IN RECENT years, electricity generation by photovoltaic (PV) or wind power (WP) has received considerable attention worldwide. The State Grid Corporation of China (SGCC) is building the National Wind/PV/battery energy storage station (BESS) and Transmission Joint demonstration project and it is located in the region of Zhangbei, Hebei, China. The Zhangbei belongs to one of the country's 10 million kilowatts of wind power base. The demonstration project is scheduled in three stages. Now, it is in the first stage and at the end of December, 2011, a 100-MW wind farm, a 40-MW PV farm, and 14-MW/63-MWh lithium-ion BESS have been built at Zhangbei.

The battery energy storage system can provide flexible energy management solutions that can improve the power quality of renewable-energy hybrid power generation systems. To that end, several control strategies and configurations for hybrid energy storage systems, such as a battery energy storage system [1]–[5], [13]–[19], a superconducting magnetic energy system (SMES) [6], a flywheel energy system (FES) [7], an energy capacitor system (ECS) [8]–[12], and a fuel cell/electrolyzer hybrid system [20], [21], have been proposed to smooth wind power fluctuation or enhance power quality. Thanks to the rapid

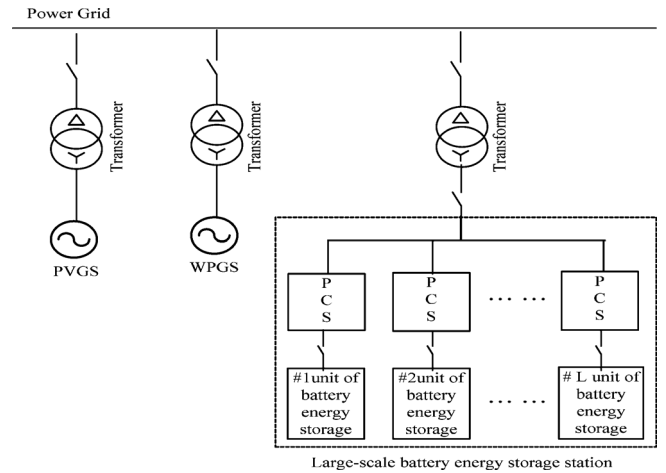


Fig. 1. Wind/PV/BESS hybrid power generation system.

development of batteries, battery energy storage systems recently have begun to be utilized for multiple applications such as frequency regulation, grid stabilization, transmission loss reduction, diminished congestion, increased reliability, wind and solar energy smoothing, spinning reserve, peak-shaving, load-leveling, uninterruptible power sources, grid services, electric vehicle (EV) charging stations, and others.

These days, the issue of how power fluctuations in PV and wind power generation are to be smoothed has attracted widespread interest and attention. And even as this issue is being resolved, another one, that of the application of an energy storage system such as BESS, has arisen. When using BESS to control PV and wind power fluctuations, there is a trade-off between battery effort and the degree of smoothness. That is, if one is willing to accept a less smooth output, the battery can be spared some effort. Thus far, although various effective BESS-based methods of smoothing power fluctuations in renewable power generation systems have been proposed [2], [3], [5], smoothing targets for grid-connected wind and PV farms generally have not been formulated. Smoothing control by way of power fluctuation rate limits, for such systems, has rarely even been discussed. The control strategies published in [1]–[5], [13]–[19], [25], [26] were formulated mainly for small-scale BESS-based smoothing; hence, they did not consider power allocation among several BESS. A suitable and effective control strategy for large-scale BESS, therefore, remains an urgent necessity.

In the present study, under the assumptions that the capacities of the WP and PV hybrid generation system (WPPVGS) and BESS had already been determined and that we do not have ability to adjust the WPPVGS output power, a large-scale BESS was used to smooth the WPPVGS output power fluctuation. More specifically, Wind/PV/BESS hybrid power generation system (Fig. 1) along with a state of charge (SOC)-based smoothing control strategy was utilized to instantaneously smoothen WP and PV power fluctuations. This was accomplished by modifying smoothed target outputs adaptively and making flexible use of feedback adjustments of battery SOC in real-time. The detailed procedure is explained in Section III.

This paper is organized as follows. Section II presents the modeling of each power source. Section III describes

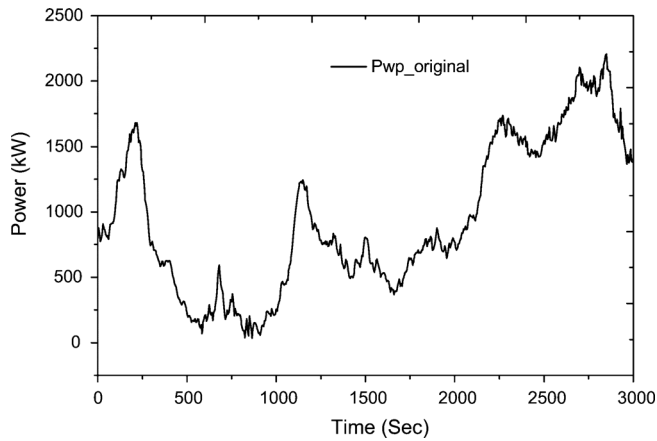


Fig. 2. WPGS power based on practically obtained wind output power at Zhangbei.

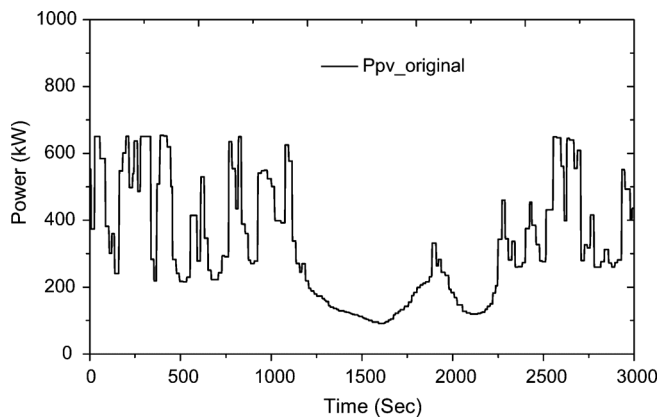


Fig. 3. PVGS power based on practically obtained PV output power at Zhangbei.

a SOC-based novel adaptive power control strategy for smoothing power fluctuations of WPPVGS output. Simulation results are discussed in Section IV through three cases. Section V is the conclusion.

II. MODELING OF POWER SOURCES

A. Modeling of Wind Power Generation System

The WP generation system shown in Fig. 2 was modeled on the 3-MW Sinovel SL3000/113 wind turbine located at the National Wind Power Integration Research and Test Center (NWIC) in Zhangbei, China. The detailed parameters of the SL3000 are available at website [22].

B. Modeling of PV Power Generation System

The PV power generation system was modeled by using practically obtained PV output power at Zhangbei. In this system, two 630-kW PCSs have been used in parallel and the rated power is 1.26 MW. The power fluctuation of the PVGS was modeled as shown in Fig. 3.

C. Modeling of BESS

A 100-kWh lithium iron phosphate (LiFePO₄) lithium-ion BESS has been modeled in reference to the R_{int} model presented in [23]–[26]. The schematic diagram of battery equivalent circuit model is shown in Fig. 4.

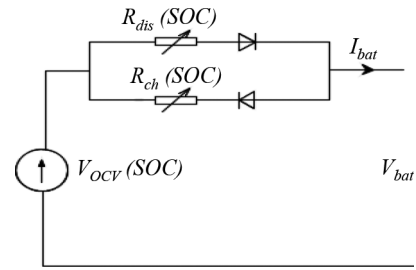


Fig. 4. Schematic diagram of battery equivalent circuit model.

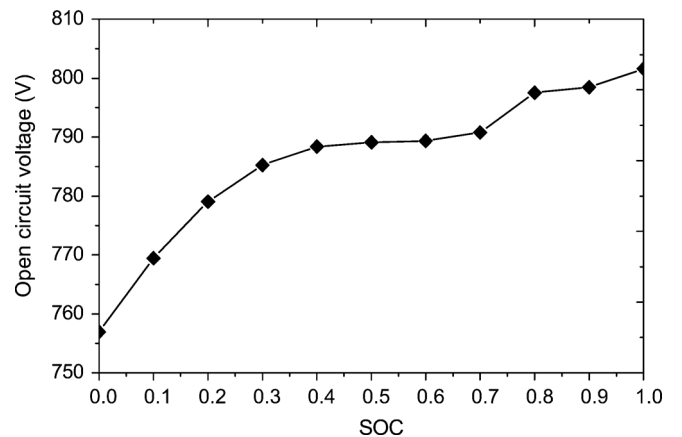


Fig. 5. Characteristic of open circuit voltage via battery SOC.

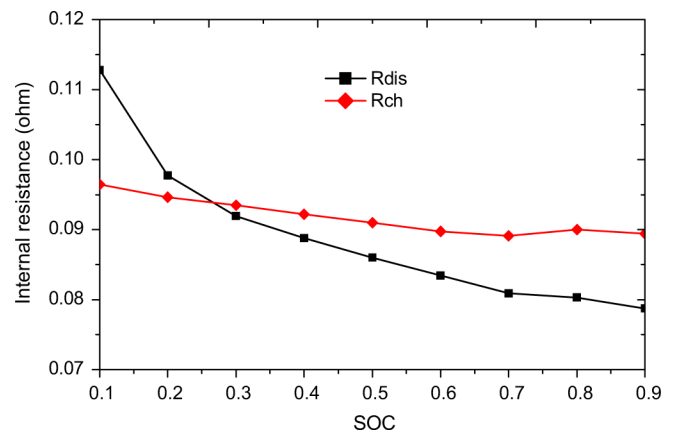


Fig. 6. Internal resistance via battery SOC.

alent circuit model is shown in Fig. 4. In general we know that V_{bat} can be expressed as (1). Moreover, as shown in (2) and (3), V_{ocv} and R_{bat}^{int} are determined by using lookup tables based on experimental data presented in Figs. 5 and 6. Fig. 5 presents characteristics of open circuit voltage via battery SOC. Fig. 6 presents internal resistance via battery SOC. The battery SOC is calculated by using (4) and (5) and the η is calculated depending on battery charging/discharging status. The charging power of BESS is indicated by the “−” symbol and the discharging power of BESS is indicated by the “+” symbol, respectively. In this paper, 1-MWh BESS is considered by integrating five 200-kWh LiFePO₄ lithium-ion BESSs in parallel. Specification of 1-MWh BESS is shown in Table I.

$$V_{bat} = V_{ocv} - R_{bat}^{int} I_{bat} \quad (1)$$

TABLE I
SPECIFICATION OF BATTERY ENERGY STORAGE SYSTEM

Index	Description
Whole system	Five 200kWh BESS in parallel
Every 200kWh BESS	two 100kWh BESS in parallel
Every 100kWh BESS	ten battery modules in series
1 module	twenty-four 120Ah single batteries in series
Single battery capacity	120Ah (two 60Ah batteries in parallel)
Rated power	5x200kW=1MW
Maximum working voltage	840V
Minimum working voltage	696V

where

$$V_{ocv} = f_1(\text{SOC}) \quad (2)$$

$$R_{\text{bat}}^{\text{int}} = \begin{cases} R_{\text{ch}} = f_2(\text{SOC}) & \text{charging} \\ R_{\text{dis}} = f_3(\text{SOC}) & \text{discharging} \end{cases} \quad (3)$$

$$\text{SOC} = \text{SOC}_{\text{ini}} - \int \frac{\eta I_{\text{bat}}}{Q_{\text{bat}}} dt \quad (4)$$

$$\eta = \begin{cases} \eta_{\text{ch}} = \frac{V_{ocv}}{V_{ocv} - I_{\text{bat}} R_{\text{ch}}} & \text{charging} \\ \eta_{\text{dis}} = \frac{V_{ocv} - I_{\text{bat}} R_{\text{dis}}}{V_{ocv}} & \text{discharging.} \end{cases} \quad (5)$$

III. SOC-BASED SMOOTHING CONTROL STRATEGY

This paper proposes a new control strategy for smoothing of wind and PV power fluctuations by means of feedback control of SOC and a large-scale BESS. First, the smoothing problem

is formulated based on the power fluctuation rate. The power fluctuation rate can be considered as an assessment indicator for PV and WP generation equipment that is connected to the power grid. As (6)–(15) indicate, the power fluctuation rates over the investigated time period are used to evaluate the control effect of PV and WP smoothing both with and without the BESS. That is, as shown in equations (6)–(15) at the bottom of the page.

In general, in order to operate the BESS continuously, the battery SOC needs to be controlled within a certain range. As a result, it can prevent the forced shutdown of the BESS due to overcharge or over-discharge of batteries. Moreover, control strategies for BESS and smoothing applications need to be developed to efficiently dispatch real-time total power demand of BESS between each PCS. Meanwhile, if the individual storage unit of SOC is higher or lower, the adaptive coordination of the smoothing level and of the power distribution between energy storage units should be considered based on the SOC and the maximum available charge or discharge power constraints of battery energy storage systems. In this paper, accordingly, the following four stages have been proposed based on the above-noted power fluctuation rate indicators for determination of the target power of the BESS and of each PCS.

1) *Stage 1: Determine Initial Target Power of BESS:* Method 1: The initial power of the BESS is calculated based on the dynamic filtering controller (DFC), as shown in the following:

$$P_{\text{BESS}}^{\text{ini}}(t) = P_{\text{WPPV}}^{\text{smooth}}(t) - P_{\text{WPPV}}(t) \quad (16)$$

$$\text{(i) If } r_{\text{WPPV}}(t) \leq \delta_{\text{WPPV}} \quad (17)$$

$$P_{\text{WPPV}}^{\text{smooth}}(t) = P_{\text{WPPV}}(t)$$

$$\text{(ii) If } r_{\text{WPPV}}(t) > \delta_{\text{WPPV}} \quad (18)$$

$$P_{\text{WPPV}}^{\text{smooth}}(t) = P_{\text{WPPV}}^{\text{smooth}}(t - \Delta t) e^{-\Delta t/T_{\text{WPPV}}} + \frac{\Delta t}{T_{\text{WPPV}}} P_{\text{WPPV}}(t).$$

$$r_{\text{WPPV}}^T = f_{\text{WPPV}} \left(\frac{P_{\text{WPPV}}^{\text{max}} - P_{\text{WPPV}}^{\text{min}}}{P_{\text{WPPV}}^{\text{rated}}} \right)_T \quad (6)$$

$$r_{\text{hybrid}}^T = f_{\text{hybrid}} \left(\frac{P_{\text{hybrid}}^{\text{max}} - P_{\text{hybrid}}^{\text{min}}}{P_{\text{WPPV}}^{\text{rated}}} \right)_T \quad (7)$$

$$P_{\text{WPPV}}^{\text{rated}} = \sum_{k=1}^W u_k^{\text{WP}} P_{\text{WP}_k}^{\text{rated}} + \sum_{k=1}^V u_k^{\text{PV}} P_{\text{PV}_k}^{\text{rated}} \quad (8)$$

$$P_{\text{WPPV}}^{\text{max}} = \max \{ P_{\text{WPPV}}(t), P_{\text{WPPV}}(t - \Delta t), \dots, P_{\text{WPPV}}[t - (n - 1)\Delta t] \} \quad (9)$$

$$P_{\text{WPPV}}^{\text{min}} = \min \{ P_{\text{WPPV}}(t), P_{\text{WPPV}}(t - \Delta t), \dots, P_{\text{WPPV}}[t - (n - 1)\Delta t] \} \quad (10)$$

$$P_{\text{hybrid}}^{\text{max}} = \max \{ P_{\text{hybrid}}(t), P_{\text{hybrid}}(t - \Delta t), \dots, P_{\text{hybrid}}[t - (n - 1)\Delta t] \} \quad (11)$$

$$P_{\text{hybrid}}^{\text{min}} = \min \{ P_{\text{hybrid}}(t), P_{\text{hybrid}}(t - \Delta t), \dots, P_{\text{hybrid}}[t - (n - 1)\Delta t] \} \quad (12)$$

$$T = n\Delta t \quad (13)$$

$$P_{\text{WPPV}}(t) = P_{\text{WP}}(t) + P_{\text{PV}}(t) \quad (14)$$

$$P_{\text{hybrid}}(t) = P_{\text{WP}}(t) + P_{\text{PV}}(t) + P_{\text{BESS}}(t) \quad (15)$$

Method 2: The initial power of the BESS is calculated based on the proposed dynamic rate limiter; that is, the rate of power change at time t is calculated by

$$r_{\text{WPPV}}(t) = \frac{P_{\text{WPPV}}(t) - P_{\text{WPPV}}(t - \Delta t)}{\Delta t}. \quad (19)$$

Then, the smoothing power is determined using the following rules:

(a) If $k_{\text{WPPV}}^{\text{drop}} \leq r_{\text{WPPV}}(t) \leq k_{\text{WPPV}}^{\text{rise}}$

$$P_{\text{WPPV}}^{\text{DRL}}(t) = P_{\text{WPPV}}(t) \quad (20)$$

(b) If $r_{\text{WPPV}}(t) > k_{\text{WPPV}}^{\text{rise}}$

$$P_{\text{WPPV}}^{\text{DRL}}(t) = P_{\text{WPPV}}^{\text{DRL}}(t - \Delta t) + \Delta t \cdot k_{\text{WPPV}}^{\text{rise}} \quad (21)$$

(c) If $r_{\text{WPPV}}(t) < k_{\text{WPPV}}^{\text{drop}}$

$$P_{\text{WPPV}}^{\text{DRL}}(t) = P_{\text{WPPV}}^{\text{DRL}}(t - \Delta t) + \Delta t \cdot k_{\text{WPPV}}^{\text{drop}}. \quad (22)$$

Further, the above-specified parameter values for the rise/drop rate limits were determined as follows:

$$k_{\text{WPPV}}^{\text{rise}} = \frac{P_{\text{WPPV}}^{\text{rated}} \times \delta_{\text{WPPV}}}{T} \quad (23)$$

$$k_{\text{WPPV}}^{\text{drop}} = -\frac{P_{\text{WPPV}}^{\text{rated}} \times \delta_{\text{WPPV}}}{T}. \quad (24)$$

Finally, the smoothing power of WP and PV generation and the initial power of the BESS were calculated as follows:

$$P_{\text{WPPV}}^{\text{smooth}}(t) = P_{\text{WPPV}}^{\text{DRL}}(t) \quad (25)$$

$$P_{\text{BESS}}^{\text{ini}}(t) = P_{\text{WPPV}}^{\text{DRL}}(t) - P_{\text{WPPV}}(t). \quad (26)$$

2) *Stage 2: Determine Target Power of Each PCS i :* The initial target power of each PCS i is calculated by using (27) and (28). If $P_{\text{BESS}}^{\text{ini}}$ is greater than zero (that is, the BESS is in discharge mode), P_i^{ini} is determined as

$$P_i^{\text{ini}} = \frac{u_i \text{SOC}_i}{\sum_{i=1}^L (u_i \text{SOC}_i)} P_{\text{BESS}}^{\text{ini}}. \quad (27)$$

If $P_{\text{BESS}}^{\text{ini}}$ is less than zero (that is, the BESS is in charge mode), P_i^{ini} is determined as

$$P_i^{\text{ini}} = \frac{u_i \text{SOD}_i}{\sum_{i=1}^L (u_i \text{SOD}_i)} P_{\text{BESS}}^{\text{ini}} \quad (28)$$

$$\text{SOD}_i = 1 - \text{SOC}_i. \quad (29)$$

3) *Determine Modified Target Power of Each PCS i :* The modified target power of each PCS is calculated by

$$\Delta P_i = A_i u_i \gamma_i \quad (30)$$

$$A_i = f_{\text{LT}}(\text{SOC}_i) \quad (31)$$

$$\gamma_i = \frac{\text{SOC}_i - \text{SOC}_{\text{ref}}}{\frac{(\text{SOC}_i^{\text{max}} - \text{SOC}_i^{\text{min}})}{2}} \quad (32)$$

$$\text{SOC}_{\text{ref}} = \begin{cases} 0.2, & \text{if } \text{SOC}_i \leq 0.1 \\ 0.8, & \text{if } \text{SOC}_i \geq 0.9 \\ \text{SOC}_i, & \text{otherwise.} \end{cases} \quad (33)$$

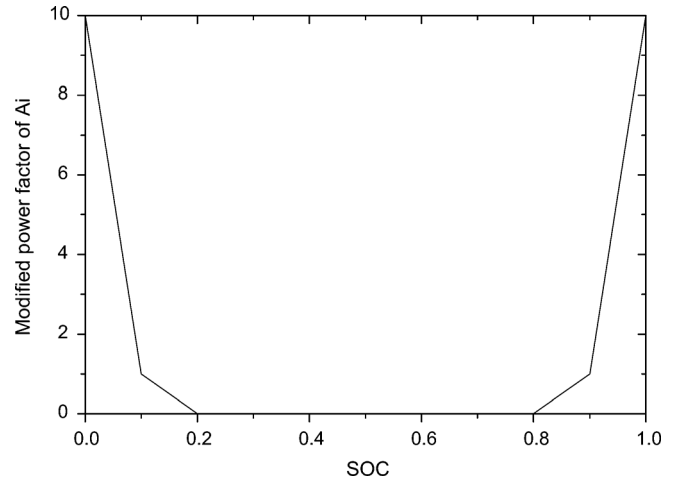


Fig. 7. Modified power factor of A_i via battery SOC.

In (30), variable A_i is mainly used to accelerate the control effect of γ_i to avoid BESS near its upper and lower limits of SOC. Fig. 7 plots the modified power factor of A_i via battery SOC that was used in the present study.

For (33), to ensure the expected status of battery SOC, a state machine is used to modify SOC_{ref} . The three states can be described as follows: 1) normal model: if the SOC is within the allowable values, SOC_{ref} is set to SOC; 2) lower limit model: if the SOC is less than $\text{SOC}_i^{\text{min}}$ [in the present study, $\text{SOC}_i^{\text{min}}$ was set to 0.1, as shown in (33)], SOC_{ref} is set to 0.2, thereby preventing the battery energy storage system from operating in the low-SOC region; 3) upper-limit model: if the SOC is larger than $\text{SOC}_i^{\text{max}}$ [in the present study, $\text{SOC}_i^{\text{max}}$ was set to 0.9, as shown in (33)], SOC_{ref} is set to 0.8, thereby preventing the battery energy storage system from operating in the high-SOC region. These functions were realized by State flow software in the present study.

4) *Stage 4: Determine Target Power for Each Unit:* With reference to the above-noted states 1 to 3, the initial power of each PCS i and that of the BESS are modified according to

$$P_i^{\text{ini-new}} = P_i^{\text{ini}} + \Delta P_i \quad (34)$$

$$P_{\text{BESS}}^{\text{ini-new}} = \sum_{i=1}^L P_i^{\text{ini-new}}. \quad (35)$$

Then, $P_i^{\text{ini-new}}$ is redetermined based on the current allowable charge/discharge power constraints for each i .

(i) If $P_{\text{BESS}}^{\text{ini-new}}$ is greater than zero (that is, the BESS is in discharge mode), $P_i^{\text{ini-new}}$ initially is sorted in descending order and is indicated by \hat{P}_j^{disch} ; then, \hat{P}_j^{disch} is refreshed, as shown in the following:

$$\hat{P}_j^{\text{disch}} = \frac{u_j \text{SOC}_j}{\sum_{j=1}^{L-M} (u_j \text{SOC}_j)} \left(P_{\text{BESS}}^{\text{ini-new}} - \sum_{i=1}^M \hat{P}_i^{\text{disch}} \right). \quad (36)$$

(ii) If $P_{\text{BESS}}^{\text{ini-new}}$ is less than zero (that is, the BESS is in charge mode), the absolute value of $P_i^{\text{ini-new}}$ initially is sorted

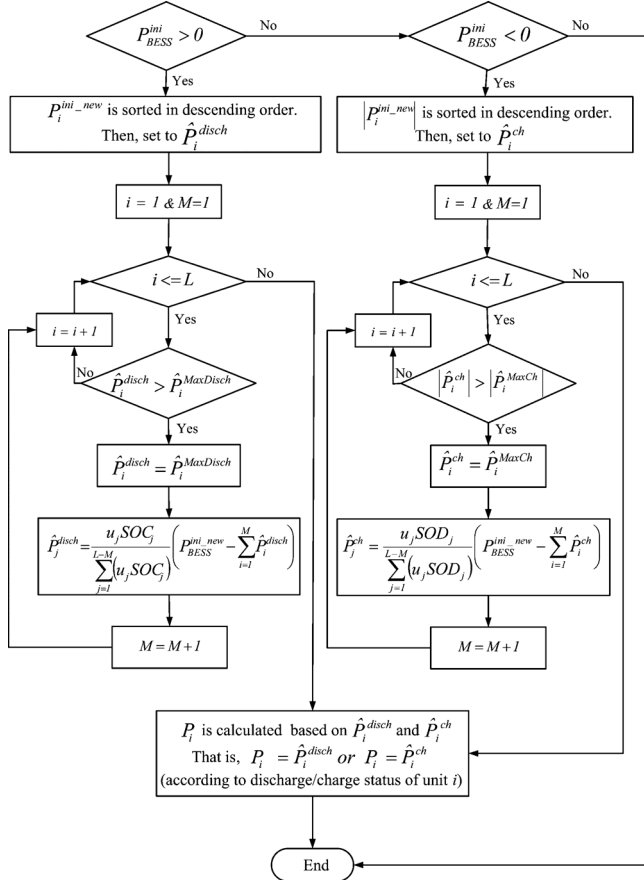


Fig. 8. Flowchart of process for meeting allowable power constraints of each BESS unit.

TABLE II
DETERMINE PCS TARGET POWER FOR 800-kW DEMAND

SOC_1	SOC_2	SOC_3	SOC_4	SOC_5
90%	70%	50%	30%	10%
$P_1^{ini_new}$	$P_2^{ini_new}$	$P_3^{ini_new}$	$P_4^{ini_new}$	$P_5^{ini_new}$
288	224	160	96	32
\hat{P}_1^{disch}	\hat{P}_2^{disch}	\hat{P}_3^{disch}	\hat{P}_4^{disch}	\hat{P}_5^{disch}
200	200	200	150	50

in descending order and is indicated by \hat{P}_i^{ch} ; then, \hat{P}_j^{ch} is renewed, as follows:

$$\hat{P}_j^{ch} = \frac{u_j SOD_j}{\sum_{j=1}^{L-M} (u_j SOD_j)} \left(P_{BESS}^{ini_new} - \sum_{i=1}^M \hat{P}_i^{ch} \right). \quad (37)$$

A detailed flowchart of the above process is provided in Fig. 8. A short numeric example to illustrate this stage 4 is shown in Tables II and III, respectively, based on 1-MWh BESS shown in Table I. A scenario of large different SOC is considered and the $P_{BESS}^{ini_new}$ is set to 800 kW and -800 kW, respectively. It can be seen that by using the proposed method, the allowable maximum discharge or charge constraint can be satisfied.

In addition, on how to determine the real-time charging and discharging power limit, the following method can be used for reference. When approaching 0% SOC, the allowable maximum

TABLE III
DETERMINE PCS TARGET POWER FOR -800 -kW DEMAND

SOC_1	SOC_2	SOC_3	SOC_4	SOC_5
90%	70%	50%	30%	10%
$P_1^{ini_new}$	$P_2^{ini_new}$	$P_3^{ini_new}$	$P_4^{ini_new}$	$P_5^{ini_new}$
-32	-96	-160	-224	-288
\hat{P}_1^{ch}	\hat{P}_2^{ch}	\hat{P}_3^{ch}	\hat{P}_4^{ch}	\hat{P}_5^{ch}
-50	-150	-200	-200	-200

discharge power of unit is set to 0 to prevent the over discharge of BESS unit. Otherwise, when approaching 100% SOC, the allowable maximum charge power of unit is set to 0 to avoid the overcharge of BESS unit.

Finally, the target power of P_i can be calculated based on \hat{P}_i^{disch} and \hat{P}_i^{ch} as shown in Fig. 8. As a result, the target power of the BESS and that of PV and WP output smoothing can be determined as follows:

$$P_{BESS} = \sum_{i=1}^L P_i \quad (38)$$

$$P_{WPPV}^{smooth} = P_{WPPV} + P_{BESS}. \quad (39)$$

IV. SIMULATION AND VALIDATION

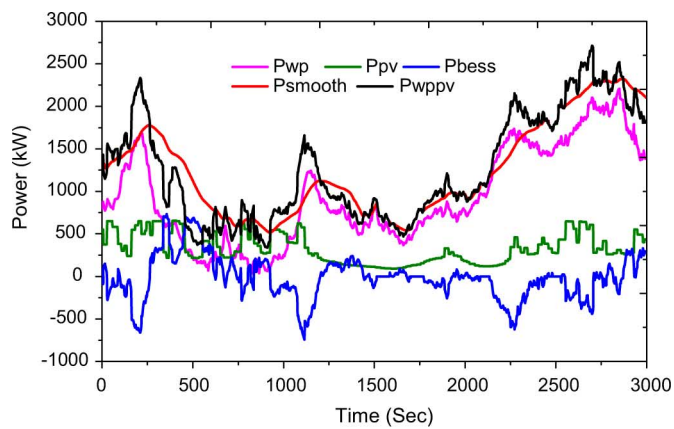
Simulation analyses were performed with a wind/PV/BESS hybrid power system model. The model integrated 3-MW WPGS, 1.26-MW PVGS, and 1-MW BESS. The BESS was connected with the WPGS and PVGS to a utility-grid power system at a common coupling point, as shown in Fig. 1. To verify the effectiveness of the proposed control strategy, a 10%–90% range of battery SOC was set, which of course was modifiable according to the BESS control requirements. A simulation test considering the following three cases was conducted with MATLAB/SIMULINK software.

A. Two Smoothing Control Methods Under Normal SOC Condition

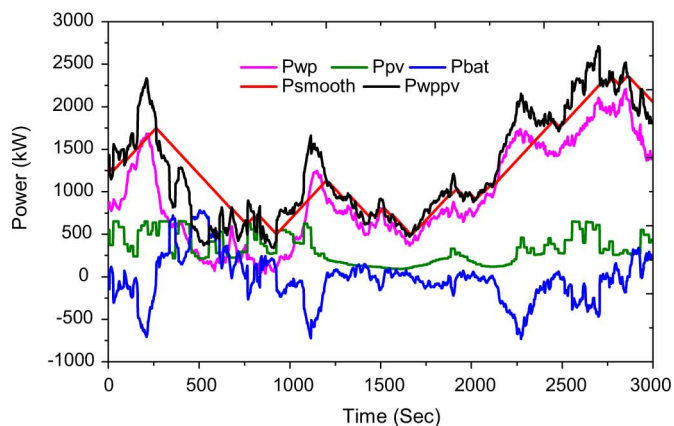
In this case, the appointed power fluctuation rate limit value of δ_{WPPV} was assumed to be 10% per 15 min. It needs to emphasize that this evaluation indicator of δ_{WPPV} should be changed according to the actual application situation. We can see that by adjusting δ_{WPPV} , the trade-off between battery effort and some degree of smoothness can be obtained. And in fact, in the actual implementation of the proposed smoothing control method, this indicator value of δ_{WPPV} should be regulated according to the connected power grid situation or actual requirements.

Then, under this assessment indicator, the two smoothing control methods were considered according to the experimental results. Additionally, for method 1, the time constant of T_{WPPV} was set to 600 s, and the allowable maximum charge/discharge power value of each unit was set to -200 kW/200 kW, respectively. It was assumed that the initial SOC of units 1, 2, 3, 4, and 5 were 60%, 55%, 50%, 45%, and 40%, respectively.

Figs. 9 and 10 show the power and power fluctuation rate profiles for the different smoothing control methods, respectively.



(a)

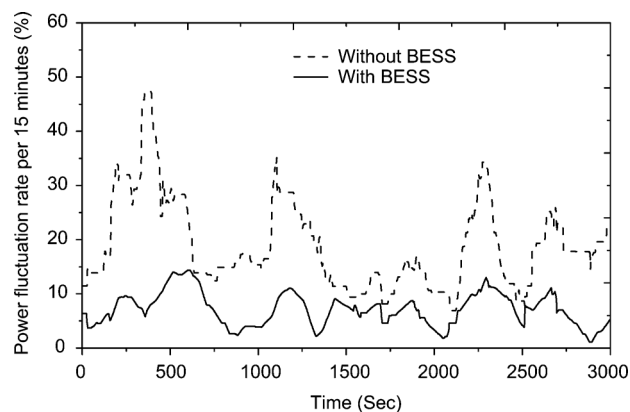


(b)

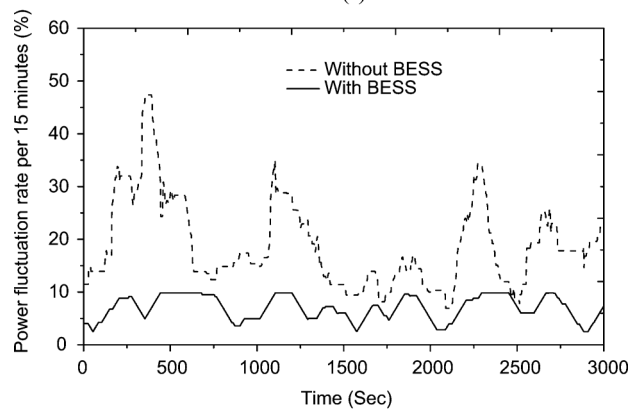
Fig. 9. Power profiles in case A (a) with method 1 and (b) with method 2.

As Fig. 9 makes clear, the control objective of the smoothing WP and PV power fluctuations could be achieved with both methods. However, Fig. 10 shows that by method 2, the hybrid WP and PV power generation fluctuations was effectively controlled below the limit value of 10% per 15 min. From the above results, we can see that the use of the control method 2 can more effectively regulate the power fluctuation rate within the specified ranges. Moreover, it should be noted that due to the inertia feature of the first-order filter, when the variable time constant control strategy has been adopted (method 1), the filter time constant needs to be modified and updated timely, otherwise, sometimes the power fluctuation rate constraint will be difficult to guarantee. However, method 2 is not only easier to be implemented, but also can ensure that when the power fluctuation rate limit value has been provided, the power fluctuation rate can be effectively controlled within a limited range. In addition, it is recommended that the limit value of the power fluctuation rate should be periodically revised based on the operational requirements of the actual on-site.

Figs. 11 and 12 show the power and SOC profiles for each PCS unit by using method 1 and method 2, respectively. As indicated in Fig. 11, the charge and discharge power of each PCS unit is adjusted in real time, based on the SOC value. That is, when the battery is in the discharging state, the battery discharge power is proportional to the SOC value; conversely, when the



(a)



(b)

Fig. 10. Power fluctuation rate profiles in case A (a) with method 1 and (b) with method 2.

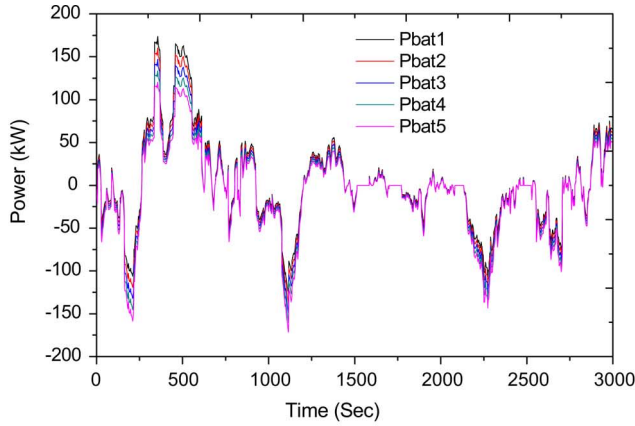
battery in the charging state, the charging power is inversely proportional to the SOC value. Moreover, as the Fig. 12 data show, the proposed smoothing control method can supervise the SOC to secure the charging level of the BESS.

B. Energy Management Under Extreme SOC Conditions

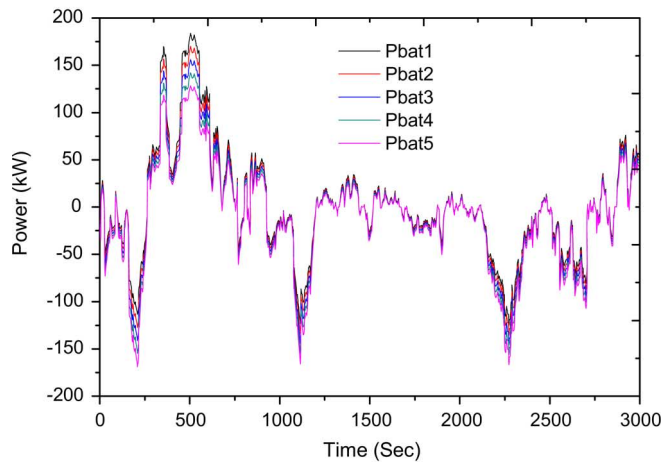
This section mainly discusses the effectiveness of the proposed BESS energy management method considering overcharge/over-discharge SOC conditions. Therefore, it was assumed that the initial SOC of units 1, 2, 3, 4, and 5 were 90%, 70%, 50%, 30%, and 10%, respectively.

Fig. 13 shows the power profile for the smoothing control method 2. The power and SOC profiles of each of the respective PCS units with method 2 are shown in Figs. 14 and 15, respectively. It is evident that, by means of the proposed control strategy, the power output fluctuations of the WPGS and PVGS hybrid system can be smoothed with extreme SOC conditions.

Moreover, as the data in Figs. 14 and 15 show, the proposed smoothing control method can supervise the SOC to secure the charging level of the BESS, specifically by adjusting each modified target power of ΔP_i for the high- and low-SOC ranges. Thereby, energy management among multiple energy storage units can be achieved and, thus, under extreme SOC conditions, by using the proposed smoothing method 2, the SOC of each unit can be effectively controlled within the specified range as shown in Fig. 15.



(a)



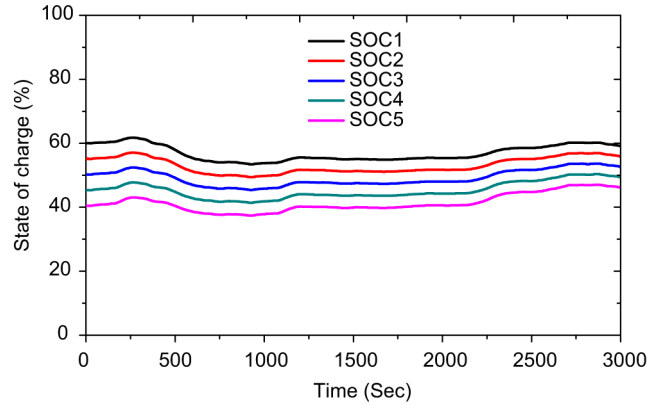
(b)

Fig. 11. Power profile for each PCS unit in Case A (a) with method 1 and (b) with method 2.

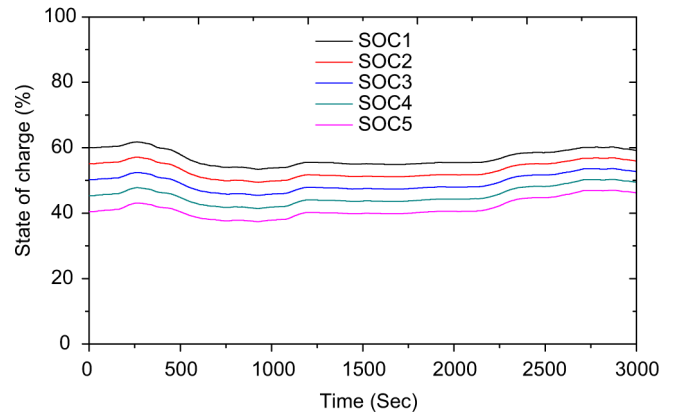
C. Daily PV Output Smoothing Control Under Power Fluctuation Rate Limit

In this case, as a special discussion, a hybrid 5-MWh BESS and large-scale PV power generation system was considered for the proposed method 2, so as to simulate a longer time covering the whole daily PV production period. The daily real PV generation data were applied, and the total rated power of the generation system was 40 MW. In this section, the 5-MWh BESS was considered by integrating five 1-MWh LiFePO₄ lithium-ion BESSs in parallel. Specification of 1-MWh BESS is presented in Table I of Section II. The allowable maximum charge/discharge power value of each 1-MWh BESS was set to -1 MW/1 MW, respectively. It was assumed that the initial SOC_s of BESS 1, 2, 3, 4, and 5 were 90%, 70%, 50%, 30%, and 10%, respectively. The appointed power fluctuation rate limit value of δ_{WPPV} was assumed once again to be 10% per 15 min.

The power profile by using proposed smoothing method 2 is plotted in Fig. 16. It can be seen that the PV power fluctuations were effectively smoothed. Fig. 17 shows the power fluctuation rate during the one-day period. As the data indicates, the proposed control strategy was effectively utilized to control the PV power fluctuation rate within the specified limit ranges while smoothing the MW-level large-scale photovoltaic power generation at the same time.



(a)



(b)

Fig. 12. SOC profiles in Case A (a) with method 1 and (b) with method 2.

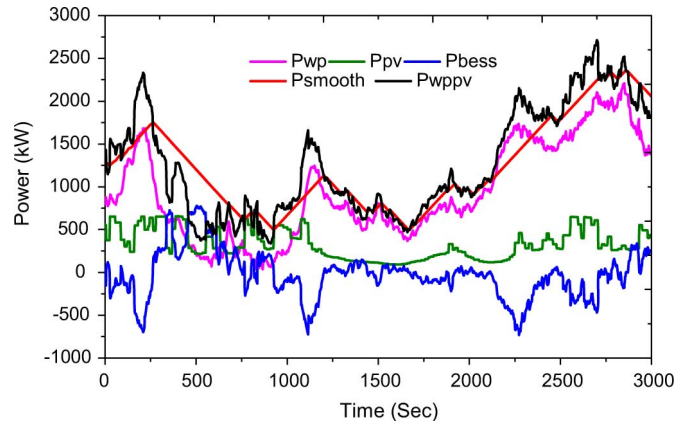


Fig. 13. Power profiles in case B.

Fig. 18 shows the SOC profiles for each 1-MWh BESS. As Fig. 18 makes clear, the proposed smoothing control method can supervise the SOC to secure the charging level of the BESS by properly allocating total power demand between each BESS.

V. CONCLUSION

The disadvantage of PV and wind power generation is their unstable power output, which can impact negatively on utility- and micro-grid operations. One means of solving this problem is to integrate PVGS and WPGS with a BESS. For such hybrid generation systems, control strategies for efficient power dispatch need to be developed. Therefore, in this paper, a novel SOC-based control strategy for smoothing the output fluctuation

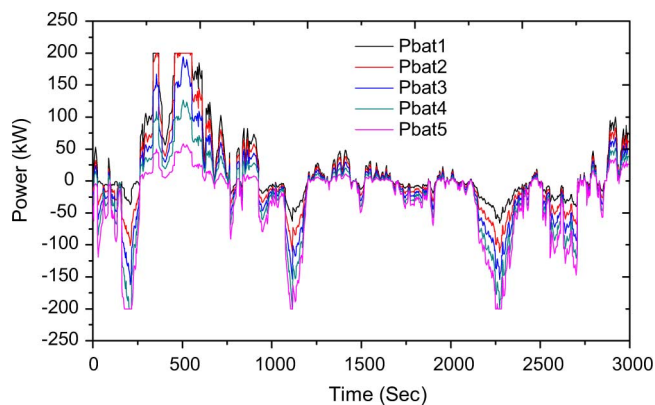


Fig. 14. Power profiles for PCS units by method 2.

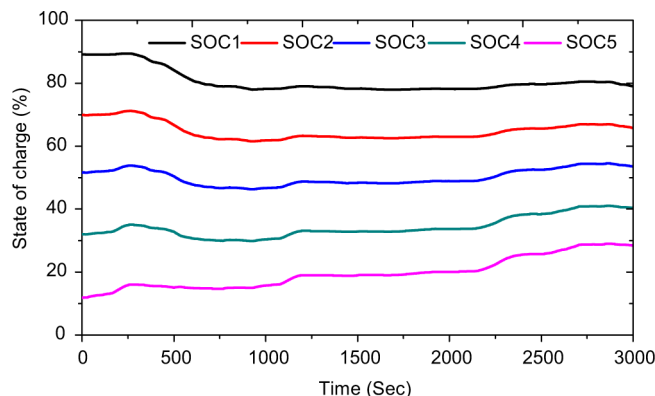


Fig. 15. SOC profiles by method 2 in Case B.

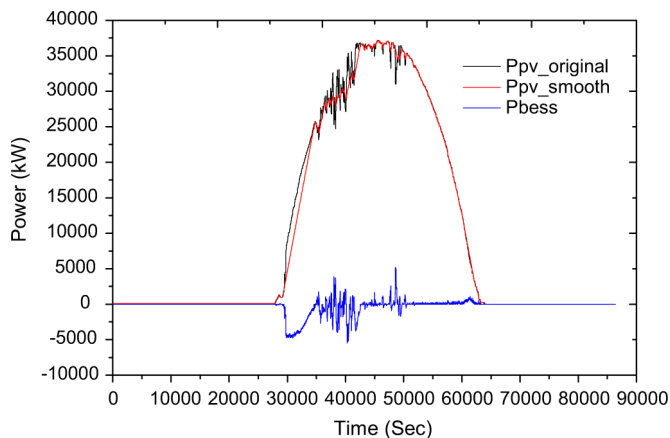


Fig. 16. Power profiles in Case C.

of a WP and PV hybrid generation system has been proposed. Additionally, the SOC feedback control strategy and the real-time power allocation method for timely regulation of battery power and energy are presented. Simulation results demonstrate that the proposed control strategy can manage BESS power and SOC within a specified target region while smoothing PVGS and WPGS outputs.

At present, how to control the SOC of the energy storage system is an ongoing research topic. We also need to combine the characteristics of the battery, and do further research and exploration. From the present research results, it can be seen that by using the proposed control method, the SOC of each battery energy storage unit can gradually move toward 50% with

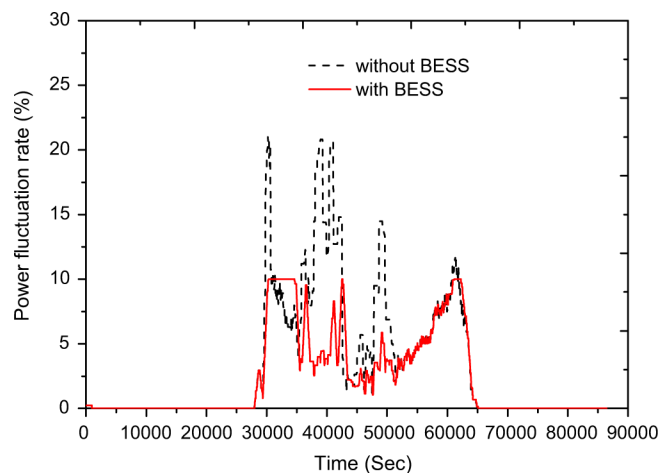


Fig. 17. Power fluctuation rates in Case C.

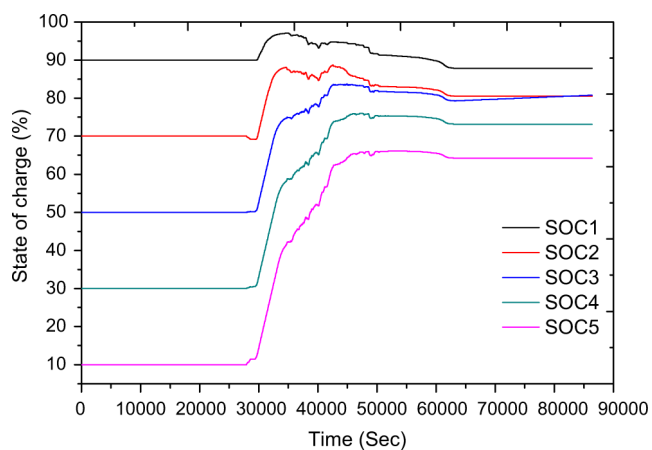


Fig. 18. SOC profiles for each BESS in Case C.

the increase of control time although the initial SOC of the energy storage unit is different. It is also considered that this control method can make the storage unit share the load as consistently as possible, so as to achieve the effect of extending the service life of the energy storage system and, therefore, can delay the accelerated decay of the battery performance. Moreover, it should be noted that some filtering on the BESS charge and discharge power have been achieved by using a power fluctuation rate constraint as the smoothing control target to prevent excessive excursions to “chase down” every PV or wind power output fluctuation.

In addition, this paper was mainly focused on the control strategies of BESS and smoothing based on battery capacity established conditions. Another significant issue is the means by which an appropriate battery capacity for this application is to be determined. The power control strategies for large-scale wind/PV/BESS hybrid power systems taking into account the optimum capacity of BESS and battery aging will be discussed in the near future combined with smoothing control application of wind and PV power generations.

REFERENCES

- [1] W. Li and J. Géza, “Comparison of energy storage system technologies and configurations in a wind farm,” in *Proc. Power Electronics Specialists Conf. (PESC 2007)*, Jun. 2007, pp. 1280–1285.

- [2] M. E. Baran, S. Teleke, L. Anderson, A. Q. Huang, S. Bhattacharya, and S. Atcitty, "STATCOM with energy storage for smoothing intermittent wind farm power," in *Proc. Power and Energy Soc. General Meeting—Conv. and Delivery of Elect. Energy in the 21st Century*, Jul. 2008, pp. 1–6.
- [3] C. Abbey, K. Strunz, and G. Joós, "A knowledge-based approach for control of two-level energy storage for wind energy systems," *IEEE Trans. Energy Convers.*, vol. 24, no. 2, pp. 539–547, Jun. 2009.
- [4] G. Koshimizu, T. Nanahara, K. Yoshimoto, H. Hasuike, and T. Shibata, "Subaru project: Application of energy storage for stabilization of wind power in power systems," in *Proc. EAS 2005 Annu. Meeting Conf. Energy Storage Assoc.*, Toronto, Canada, 2005.
- [5] K. Yoshimoto, T. Nanahara, and G. Koshimizu, "New control method for regulating state-of-charge of a battery in hybrid wind power/battery energy storage system," in *Proc. IEEE Power Syst. Conf. and Exposition*, 2006, pp. 1244–1251.
- [6] F. Zhou, G. Joos, C. Abbey, L. Jiao, and B. T. Ooi, "Use of large capacity SMES to improve the power quality and stability of wind farms," in *Proc. IEEE Power Eng. Soc. General Meeting*, Jun. 2004, pp. 2025–2030.
- [7] R. Cardenas, R. Pena, G. Asher, and J. Clare, "Power smoothing in wind generation systems using a sensorless vector controlled induction machine driving a flywheel," *IEEE Trans. Energy Convers.*, vol. 19, no. 1, pp. 206–216, Mar. 2004.
- [8] S. M. Mueeen, R. Takahashi, T. Murata, and J. Tamura, "Integration of an energy capacitor system with a variable-speed wind generator," *IEEE Trans. Energy Convers.*, vol. 24, no. 3, pp. 740–749, Sep. 2009.
- [9] S. M. Mueeen, R. Takahashi, M. H. Ali, T. Murata, and J. Tamura, "Transient stability augmentation of power system including wind farms by using ECS," *IEEE Trans. Power Syst.*, vol. 23, no. 3, pp. 1179–1187, Aug. 2008.
- [10] H. Fakhm and D. L. B. Francois, "Power control design of a battery charger in a hybrid active PV generator for load-following applications," *IEEE Trans. Ind. Electron.*, vol. 58, no. 1, pp. 85–94, Jan. 2011.
- [11] R. Kamel, A. Chaouachi, and K. Nagasaka, "Wind power smoothing using fuzzy logic pitch controller and energy capacitor system for improvement micro-grid performance in islanding mode," *Energy*, vol. 35, pp. 2119–2129, 2010.
- [12] T. Kinjo, T. Senjyu, N. Urasaki, and H. Fujita, "Output levelling of renewable energy by Electric double-layer capacitor applied for energy storage system," *IEEE Trans. Energy Convers.*, vol. 21, no. 1, pp. 221–227, Mar. 2006.
- [13] S. M. Mueeen, R. Takahashi, T. Murata, J. Tamura, and M. H. Ali, "Application of STATCOM/BESS for wind power smoothing and hydrogen generation," *Electric Power Syst. Res.*, vol. 79, no. 2, pp. 365–373, Feb. 2009.
- [14] S. Teleke, M. E. Baran, A. Q. Huang, S. Bhattacharya, and L. Anderson, "Control strategies for battery energy storage for wind farm dispatching," *IEEE Trans. Energy Convers.*, vol. 24, no. 3, pp. 725–732, Sep. 2009.
- [15] J. Zeng, B. Zhang, C. Mao, and Y. Wang, "Use of battery energy storage system to improve the power quality and stability of wind farms," in *Proc. Int. Conf. Power Syst. Technol. (Power Con 2006)*, Oct. 2006, pp. 1–6.
- [16] C. Wang and M. H. Nehrir, "Power management of a stand-alone wind/photovoltaic/fuel cell energy system," *IEEE Trans. Energy Convers.*, vol. 23, no. 3, pp. 957–967, Sep. 2008.
- [17] N. Kawakami, Y. Iijima, Y. Sakanaka, M. Fukuhara, K. Ogawa, M. Bando, and T. Matsuda, "Development and field experiences of stabilization system using 34 MW NAS batteries for a 51 MW wind farm," in *Proc. IEEE Int. Symp. Ind. Electronics (ISIE2010)*, Jul. 2010, p. 2371.
- [18] K. Takigawa, N. Okada, N. Kuwabara, A. Kitamura, and F. Yamamoto, "Development and performance test of smart power conditioner for value-added PV application," *Solar Energy Materials & Solar Cells*, vol. 75, pp. 547–555, 2003.
- [19] X. Li, D. Hui, L. Wu, and X. Lai, "Control strategy of battery state of charge for wind/battery hybrid power system," in *Proc. IEEE Int. Symp. Ind. Electronics (ISIE2010)*, Bari, Jul. 2010, pp. 2723–2726.
- [20] X. Li, S. Yu-Jin, and H. Soo-Bin, "Study on power quality control in multiple renewable energy hybrid micro grid system," in *Proc. IEEE Power Tech 2007*, Jul. 2007, pp. 2000–2005.
- [21] X. Li, Y.-J. Song, and S.-B. Han, "Frequency control in micro-grid power system combined with electrolyzer system and fuzzy PI controller," *J. Power Sources*, vol. 180, no. 1, pp. 468–475, May 2008.
- [22] SL3000 [Online]. Available: http://www.cwei.org.cn/windpowerfor/Product_Content.aspx?ID=40
- [23] X. Li, L. Xu, J. Hua, X. Lin, J. Li, and M. Ouyang, "Power management strategy for vehicular-applied hybrid fuel cell/battery power system," *J. Power Sources*, vol. 191, no. 2, pp. 542–549, Jun. 2009.
- [24] X. Li, J. Li, L. Xu, M. Ouyang, X. Han, L. Lu, and C. Lin, "Online management of lithium-ion battery based on time-triggered controller area network for fuel cell hybrid vehicle applications," *J. Power Sources*, vol. 195, no. 10, pp. 3338–3343, May 2010.
- [25] X. Li, Y. Li, X. Han, and D. Hui, "Application of fuzzy wavelet transform to smooth wind/PV hybrid power system output with battery energy storage system," *Energy Procedia*, vol. 12, pp. 994–1001, 2011.
- [26] X. Li, "Fuzzy adaptive Kalman filter for wind power output smoothing with battery energy storage system," *IET Renew. Power Generat.*, vol. 6, no. 5, pp. 340–347, Sep. 2012.



Xiangjun Li (M'06–SM'12) was born in 1979. He received the B.E. degree in electrical engineering from Shenyang University of Technology, China, in July 2001, and the M.E. and Ph.D. degrees in electrical and electronic engineering from Kitami Institute of Technology (KIT), Japan, in March 2004 and March 2006, respectively.

From May 2006 to March 2010, he worked as a postdoctoral research fellow at Korea Institute of Energy Research (KIER), Daejeon, Korea, and Tsinghua University, Beijing, China, respectively. In March 2010, he joined the Electrical Engineering and New Material Department, China Electric Power Research Institute (CEPRI), Beijing, China, where he has been engaged in the topic of integration/control/SCADA/application technologies for large-scale multitype battery energy storage systems/stations, wind/PV/battery hybrid distributed generation systems, and micro-grids. His research interests include renewable energy power generation, electric energy saving/storage technology, and power system engineering.

Dr. Li is a senior member of CES and a member of IET and IEEE.



Dong Hui received the B.S. and M.S. degrees in semiconductor physics and devices from Huazhong University of Science and Technology, China, in 1990 and 1995, respectively, and the Ph.D. degree in applied superconductivity from the Institute of Electrical Engineering, Chinese Academy of Sciences, in 1998.

He worked as a visiting scientist at Deutsches Elektronen Synchrotron (DESY), Hamburg, Germany, from May 1999 to May 2002. After that, he worked as associate professor, at the Institute of Electrical Engineering, Chinese Academy of Sciences, from May 2002 to May 2007. He has been a professor at the China Electric Power Research Institute since June 2007 and is now the Chief Engineer of Electrical Engineering and New Material Department of CEPRI. His research interests include large scale battery energy storage and power electronics.



Xiaokang Lai received the M.S. degree from China Electric Power Research Institute (CEPRI) in 1984.

He has been a Director at the Electrical Engineering Department of CEPRI since 2006. He has worked as a vice chairman of the Energy Industry Flow Battery Standardization Committee from 2012. His research interests include electrical new technology and high voltage engineering. He has made outstanding contributions in research fields such as energy storage technologies, electric vehicles, and applied superconductivity, etc.

Prof. Lai is a winner of the Third Prize of the National Science and Technology Progress Award.